medRxiv preprint doi: https://doi.org/10.1101/2020.10.12.20211094; this version posted October 14, 2020. The copyright holder for this preprint (which was not certified by peer review) is the author/funder, who has granted medRxiv a license to display the preprint in perpetuity.
It is made available under a CC-BY-NC 4.0 International license .

Prioritisation of population groups with the most interactions for COVID-19 vaccination can substantially reduce total fatalities

Jorge Rodríguez[1,2*], Mauricio Patón[1] and Juan M Acuña[2]

[1]Department of Chemical Engineering. College of Engineering. Khalifa University.
SAN Campus PO Box 2533 Abu Dhabi, United Arab Emirates

[2]Department of Epidemiology and Public Health. College of Medicine. Khalifa University.
PO Box 127788 Abu Dhabi, United Arab Emirates

[*]Corresponding author: *jorge.rodriguez@ku.ac.ae*

Abstract

The rapid development of vaccines against the SARS-CoV-2 virus is an unprecedented achievement. Once vaccines become mass produced, they will have to be distributed to almost the entire population to prevent deaths and permit prompt economic recovery. The necessity to vaccinate a large number of people in a short period of time, and possibly with insufficient vaccine doses to cover most, creates in itself a new challenge for governments and health authorities: which population groups (by age or other criteria) should be targeted first and what sequence must be followed, if any at all, to achieve the minimum number of fatalities? In this work, we demonstrate the importance and impact of optimally planning the priorities for vaccine deployment by population groups using a modified SEIR-type model for the COVID-19 outbreak considering age-related groups. Finding the absolute guaranteed best solution of the mathematical optimisation problem may be hard, if even possible, and would likely require intense computational resources for every possible case study scenario. In this work, several strategies are evaluated and compared, in an attempt to approach the most effective possible vaccination priority sequence in an example case study using demographic and epidemiological data from Spain. The minimum total fatalities at the end of the vaccination campaign is the objective pursued. The population groups classifications are established based on relevant differences in mortality (due to their age) and risk-related behaviour such as their number of daily person-to-person interactions. Assuming a capacity limited constant vaccination rate, vaccination distribution strategies were evaluated for different vaccine effectiveness levels and different percentages of final vaccine population coverage. Our results unambiguously show how planning vaccination by priority groups can achieve dramatic reductions in total fatalities (more than 70% in some cases) compared to no prioritisation. The results also indicate in all cases, for all vaccine effectiveness and coverage values evaluated, that the criteria for groups vaccination priority should not be those with the highest mortality but rather those the highest number of daily person-to-person interactions. Strikingly, our results show in all cases, that prioritisation of groups with the highest mortality but less social interactions, may lead to significantly larger numbers of final total fatalities, even higher as if no group priorities were established at all. The explanation, clearly displayed by the mechanistic model, is that vaccination avoids infections that reduce mortality not only from the vaccinated group itself but also from the projected secondary and subsequent infections inflicted on the rest of the population by those vaccinated in that group. Precisely this amplification effect (exponential nature of the curve) appears to cause the larger reduction in total fatalities if the groups with the most interactions are vaccinated first. The possible contradiction of these results with some published recommendations highlight the importance of conducting an open comprehensive and rigorous analysis of this problem leaving behind any subjective preconceptions.

NOTE: This preprint reports new research that has not been certified by peer review and should not be used to guide clinical practice.

medRxiv preprint doi: https://doi.org/10.1101/2020.10.12.20211094; this version posted October 14, 2020. The copyright holder for this preprint (which was not certified by peer review) is the author/funder, who has granted medRxiv a license to display the preprint in perpetuity.
It is made available under a CC-BY-NC 4.0 International license .

Introduction

COVID-19 has inflicted great stress worldwide with more than 37 million cases and 920 thousand deaths globally as of October 12, 2020. (JHCRC 2020). Despite a tendency to a decrease in the number of cases per day in many countries, and even regions in the world, the pandemic is not near its end and the disease will probably not go away, becoming endemic in many regions throughout the world. In this scenario, the development of adequate vaccines is an alternative for primary prevention of the disease, so far implemented through hygiene, social isolation, social distancing, and quarantine. Vaccines then are the next best hope for the world in the COVID-19 pandemic.

Vaccines, of different types, are products of biotechnological processes and their development and approval is long, taking on average several years. This was the rule until now: in an unprecedented global effort from pharma and academia, supported by government and private organizations, streamlined regulation and financial investment have made possible that one or more COVID-19 vaccines may become available during early 2021. Although the tremendous speed with which COVID-19 vaccines are being approved and trials implemented, and the scientific world concerns about the science, the politics, and the economics of such speedy processes, it is probably unavoidable that one or more vaccines will become available soon.

With more than 320 candidates and 76 trials now underway (15 in phase I; 25 in phase I/II; 4 in phase II; 2 in phase II/III; and 13 in phase III), registered at ClinicalTrials.gov, the next problems to sort out will probably be mass production of the vaccine and how to determine the vaccine availability for potential users. (Krammer 2020; Parker *et al*., 2020).

The WHO issued a draft statement on September 9, 2020, addressing issues related to the fair allocation of vaccines for countries around the world. Available doses of COVID-19 vaccines worldwide are proposed to be managed centrally and equitably by the COVAX Access Mechanism, a coalition of member countries together with the ACT-Accelerator Collaboration (WHO; the Bill & Melinda Gates Foundation; Gavi, the Vaccine Alliance; the Global Fund; the Coalition for Epidemic Preparedness Innovations -CEPI; and Welcome Trust) (WHO, 2020a) to allow fair allocation of available vaccines. However, in the same statement, the country allocation of vaccines provided to each one of the countries will be driven by each country itself.

Despite the estimated and unprecedented fast production of vaccines, and mostly due to the immense need for potential users (the vast majority of the population worldwide is still susceptible to the infection), vaccines provided will be insufficient. The COVAX initiative (WHO 2020a) proposes vaccine doses for each country to cover 3% to 20% of the population proportionally to each country, in two phases. However, it specifically does not address intra-country distributions for each country's population. And despite adequate world-wide equitable distribution, the final impact of the vaccine administration to populations will be dependent then, only on the internal country distribution specifically. With the limited availability forecasted (having the capacity of progressively covering 3 to 20% of the population for most countries) the internal distribution within each country becomes paramount in the final effect of the vaccination campaign for COVID-19 and the impact it will have in each country population. There is no doubt that vaccine uptake will be an important driver (Mello *et al*., 2020) however, intra-country capacity for adequate vaccine distribution will be essential and will most likely impact the final amount of deaths related to COVID-19 (Schwartz 2020).

Some of the important drivers for vaccine allocation seem to rise from ethical principles. (Field *et al*., 2012; Liu *et al*., 2020). For instance, as stated by Emmanuel *et al*.(2020), these ethical principles point towards first, reducing premature deaths; then, reducing economic and social serious deprivations and last, focus on return to functional populations and societies. However, as disputed the order and scope of these principles may be, we do agree that the immediate need of decreasing COVID-19 deaths (direct and indirect) that may be avoidable, is the first priority.

medRxiv preprint doi: https://doi.org/10.1101/2020.10.12.20211094; this version posted October 14, 2020. The copyright holder for this preprint (which was not certified by peer review) is the author/funder, who has granted medRxiv a license to display the preprint in perpetuity.
It is made available under a CC-BY-NC 4.0 International license .

The empiric decisions in a pandemic are a luxury not always possible. In these cases, mathematical modelling might guide immediate decisions, such as the impact of non-pharmaceutical interventions (Rodríguez *et al*. 2020) or in this case vaccine prioritization, fundamentally based on trying to avoid premature, preventable deaths. Under stable conditions of capacity and resources, and the capacity of public health systems to adapt to COVID-19 (WHO 2020b), these deaths (in number) are linked to the number of cases and the severity of disease: the more cases and the more severe they are, the higher the number of deaths. The number of cases, in turn, is related to the serial interval (usually stable throughout the infection) (Nishiura *et al*., 2020) and the Reproductive Number (R_0) of the disease, or better, the effective Reproductive Number (R_t) if we consider this indicator an active one as opposed to a passive one) (Cori *et al*., 2020). Most countries have managed statistics for COVID-19, the number of factors involved in the calculation of R_t and of the number of deaths is complex due to multifactorial associations of factors causing deaths. Also vaccination will change in real-time the characteristics of the population, changing the R_t and the probability of death as time elapses in the vaccination campaigns. It is easy to conclude then that in view of this, a fixed approach during a prolonged amount of time during for vaccine distribution within countries, will not produce the best possible results in averting the highest potential number of preventable deaths by vaccination.

The COVID-19 outbreak has brought unprecedented attention to mathematical modelling, with the development of several epidemic models trying to forecast the extent of the pandemic (Gatto *et al*., 2020; Giordano *et al*., 2020; Hellewell *et al*., 2020; Kissler *et al*., 2020; Kucharski *et al*., 2020; Roosa *et al*., 2020; Wilder *et al*., 2020). Some previous SEIR models already evaluated vaccination strategies for infectious diseases (Wang *et al*., 2019; Yu *et al*., 2016). Due to the attention drawn from the COVID-19 outbreak, additional models have been developed to evaluate vaccination strategies against SASRS-CoV-2. The goal of these models is to elucidate which strategy might be best for vaccinating the population with the objective of reducing the number of fatalities and/or hospitalized people (Bubar *et al*., 2020; Matrajt *et al*., 2020). Mathematical models of the COVID-19 vaccination that allow for the input of real-time information can be important to minimise the number of fatalities. By using such models, the vaccination campaigns may change directionality in allocation as needed and as indicated by the changing characteristics of the population due to the vaccination itself.

In this work, a new COVID-19 SEIR-type model, based on that by Rodríguez *et al*. (2020) segregated by population groups, is applied to solve the problem of determining the best sequence of priority population groups that should be followed for vaccination. Although slightly different optimisation goals are possible, in this work the minimum total fatalities at the end of the vaccination campaign is the pursued goal. Model-based optimisation is applied to an example with demographic and epidemiological data from Spain.

Dynamic model of the COVID-19 outbreak including vaccination

In our previous work (Rodríguez *et al*., 2020) a model was developed to describe the impact of interventions with population groups segregated by age. The model, originally designed to evaluate the impact of a number of interventions on the outbreak dynamics and outcome, captures the differences in severity, mortality and infection risk-related behaviour of different population groups by age. Based on that work a new model is presented suitable for its application to the problem of optimum vaccine allocation optimisation at hand. In the new model, the individuals are segregated by population groups, still related to their age, however other arbitrary classifications based on their activity and epidemiological differences are also possible. This could include groups such as front line workers, individuals with a very high risk of mortality etc. Individuals in the population belong

medRxiv preprint doi: https://doi.org/10.1101/2020.10.12.20211094; this version posted October 14, 2020. The copyright holder for this preprint (which was not certified by peer review) is the author/funder, who has granted medRxiv a license to display the preprint in perpetuity.
It is made available under a CC-BY-NC 4.0 International license .

to only one single group that they never abandon and transition through infection severity stages eventually joining the immune recovered pool.

Figure 1 provides a graphical representation of the different stages and transitions among them for the individuals in the different (age-related) population groups. The incorporation of vaccination causes individuals to transition to vaccinated immune or to ineffectively vaccinated not-immune stages. A complete comprehensive description of the model is presented in the Appendix including complete detailed reproducible descriptions of all equations, variables and parameters.

The model classifies individuals in the population in compartments by infection stage and (age-related) population group. In order to ensure maximum utilisation of information, either available or measurable and to minimise uncertainty, the population grouping should be defined, and it is in this case, based on meaningful epidemiological differences between individuals in severity and mortality as well as in behaviour or activity traits affecting risk of infection. These later could include traits such as the number and types (with which other groups) of daily contacts, their differences in awareness and protection attitudes, etc. The rates of infection and vaccination, together with the available recent clinical and epidemiological information, govern the transitions of individuals between disease stages and allow for the evaluation of the objective function of total fatalities at the end of the vaccination campaign. The model implementation can be fully customised with the specific population characteristics and parameters of any community, region or country for its application to determine their optimum vaccination plan.

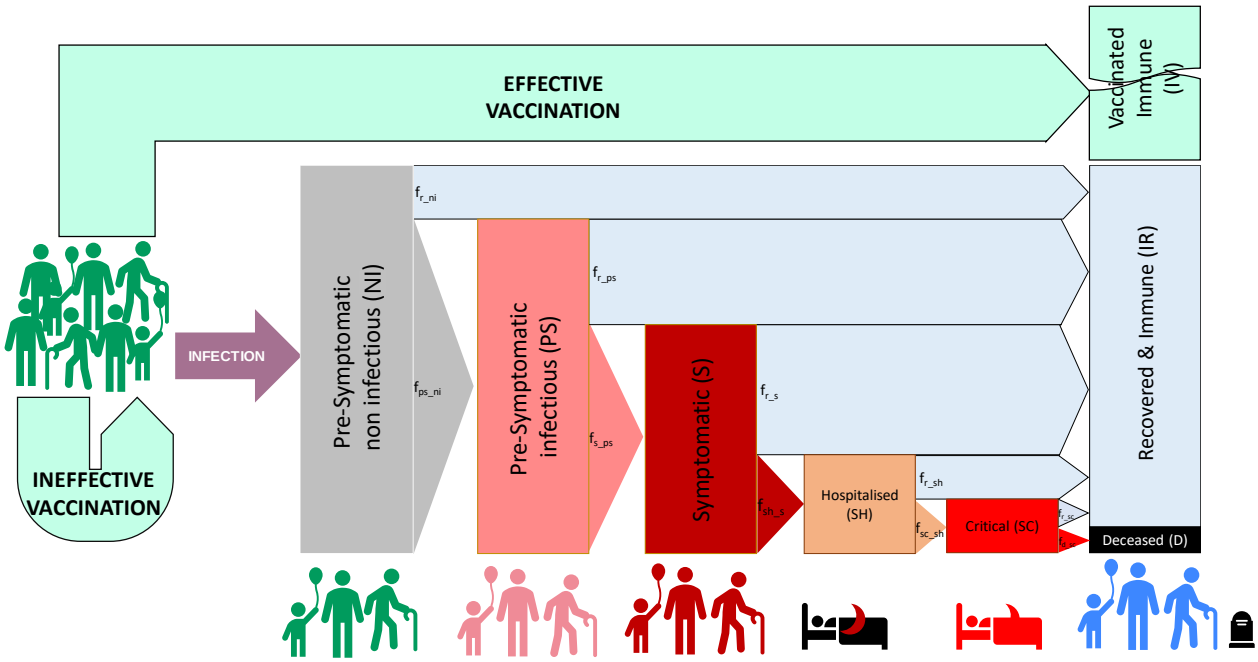

Figure 1. Representation of the model transitions of individuals through the infection stages. Only contacts of healthy susceptible individuals with infectious either pre-symptomatic or symptomatic individuals can lead to infection. Vaccination, if effective, avoids infection and places individuals at immune vaccinated stage. Ineffective vaccination maintains individuals in their current stage (they are however accounted separately as already vaccinated).

In the example to be presented for Spain, population groups were defined by (age-related) activity as namely: *preschool children* (ages 0-4); *school children* (ages 5-14); *higher school and university young* (ages 15-24), *young workers* (ages 25-49); *mature workers* (ages 50-59); *senior workers* (ages 60-64); *early retired* (ages 65-69); *retired* (ages 70-79); *elderly* (ages 80+). This groups' definition is arbitrary but it takes into account the above mentioned criteria for group definitions

medRxiv preprint doi: https://doi.org/10.1101/2020.10.12.20211094; this version posted October 14, 2020. The copyright holder for this preprint (which was not certified by peer review) is the author/funder, who has granted medRxiv a license to display the preprint in perpetuity.
It is made available under a CC-BY-NC 4.0 International license .

for impact on the final objective. The group definitions can be changed to best suit any country or region specifics, as long and good quality data are available for their characterisation.

Individuals never leave the (age-related) population group to which they belong and, at a given time, they sit on one of the possible infection stages. These stages are defined in terms of infectiousness and severity of symptoms analogously as in Rodríguez *et al*. (2020), namely: *healthy susceptible* (H); *infected non-symptomatic non-infectious* (NI); *pre-symptomatic infectious* (PS); *symptomatic infectious* (S); *in need of hospitalisation* (SH); *in need of critical care* (SC); *recovered immune* (IR) and *deceased* (D), in addition those effectively vaccinated become *vaccinated immune* (V). Individuals ineffectively vaccinated (i.e. the vaccine does not immunise them) maintain their current stage and they are simply accounted as is that stage but already vaccinated (see Figure 1).

The transitions between stages are determined by rates of infection, disease progression and vaccination. Figure 2 provides an overview representation of the stage transitions as modelled. Complete details are included in the Appendix model description

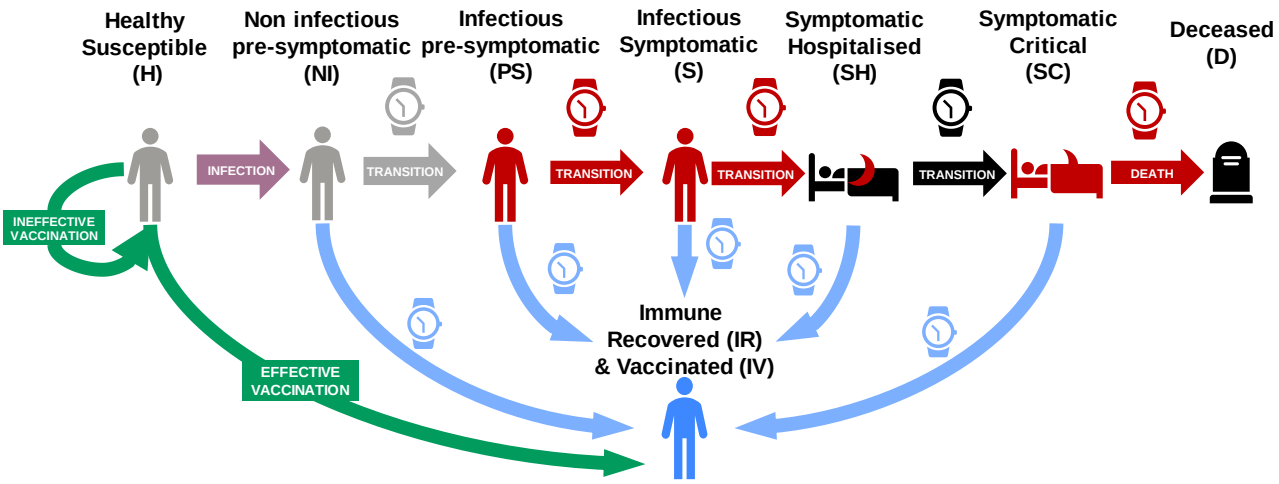

Figure 2. Schematic representation of the transition rates between stages. Individuals spend in each stage an average amount of time depending on their transition path towards recovery or increased severity.

Model limitations and assumptions

The model presented above and fully described in the Appendix was specifically developed for the optimum vaccination problem at hand. The model shares many of the fundamental characteristics of compartment SEIR-type models and its limitations remain similar as for earlier models (Rodríguez *et al*., 2020). It is based on dynamic balances of individuals in compartments classified by their stage of infection and segregated by age-related groups. In this type of models all individuals are considered located in a common single domain or closed community (e.g. a well-mixed city or town).

The model is completely deterministic, has a moderate complexity and is computationally inexpensive to solve and requires only parameters that are mechanistic and carry meaning and interpretation. Most of these parameters can be directly estimated from epidemiological and clinical data and their calibration is not recommended. Analogous to similar compartmental SEIR-type models, variables and parameters refer to representative averages for each compartment stage and population group. These characteristics may limit the model representation of non-linear relevant phenomena that may occur in the real-world reality. Examples of these include phenomena like the so-called super spread events or other location specific phenomena and cannot be captured by these types of models. Any quantitative application of the model for prediction purposes in public health should be accompanied by a critical discussion against these limitations (Wearing *et al*., 2005).

medRxiv preprint doi: https://doi.org/10.1101/2020.10.12.20211094; this version posted October 14, 2020. The copyright holder for this preprint (which was not certified by peer review) is the author/funder, who has granted medRxiv a license to display the preprint in perpetuity.
It is made available under a CC-BY-NC 4.0 International license .

No geographical clustering or separation, neither any form of migration in or out of the community are captured by this type of models. Large cities with ample use of public transportation remain the best described by this and other SEIR-type disease propagation models. The model, as described above and in full in the Appendix, is applied under specific assumptions, relevant to the vaccination problem at hand, including:

✓ All ever-infected individuals that recover become fully immune, irrespective of their severity path, and cannot be infected or infectious again.

✓ No differences in immunity or any other epidemiological aspect are considered between individuals never vaccinated and those ineffectively vaccinated.

✓ Recovered individuals (aware or not) are equally eligible for vaccination as healthy susceptible.

✓ The rates of vaccination of the groups activated (i.e. called for vaccination) are proportional to their relative sizes in terms of eligible individuals pending vaccination. The total vaccination rate must match the given rate limited by the capacity of the health system.

Optimisation of the vaccine deployment by population groups

In order to find the optimum sequence of vaccination in terms of which population groups should be targeted at each specific moment, it is necessary to solve an optimisation problem. All optimisation problems consist of a target objective to make minimum (e.g. number of total fatalities at the end of the campaign) and a set of decision variables that can be manipulated to achieve that, in this case the populations groups called for vaccination at any given time. Once the problem is defined, the optimum set of decision variables is computationally sought following a suitable existing optimisation method from literature or developed *ad hoc*. The nature of the optimisation problem at hand falls within an type of problems called dynamic programming problems. In this type of problems as it is the case here, the decision variables (in our case the active groups called for vaccination as defined in the $\boldsymbol{f_v}$ vector of ones and zeros) are not constant but change over time. This adds additional potential complexity as not only an optimum group or set of groups needs to be found but this needs to be done at each moment and changes in time. For a specific period one group(s) may the optimum target but, after some time, another group(s) may become the most useful to target for vaccination.

Objective function – Optimisation goal

Several different objective functions can be defined for minimisation depending on the priorities followed. In the example case study presented, the objective will be to minimise the total number of fatalities at one month after the vaccination campaign is completed (t_f). The definition of the optimisation problem will therefore consist of

$$\text{Minimise } \Sigma_i N_d^i(t_f) \text{ as a function of the dynamic values of } f_v^i(t)$$

$$\text{such that } \forall t \in [0,t_f] \text{ , } f_v^i \in \{0,1\}$$

Alternative formulations of the objective function are possible, for example, the total number of years of healthy life lost at (t_f) could be the target to minimise or even factoring economic losses or other terms of relevance to public health could be included. There is ample flexibility to define the problem as convenient using this framework and model.

The model itself allows for the simultaneous dynamic optimisation of vaccination together with the application of interventions over time (such as e.g. isolation of specific groups) and therefore can applied to evaluate specific scenarios combining interventions and vaccination strategies.

A plethora of optimisation approaches can be proposed and attempted to achieve the best possible results given this and any optimisation problem. These methods can be completely

medRxiv preprint doi: https://doi.org/10.1101/2020.10.12.20211094; this version posted October 14, 2020. The copyright holder for this preprint (which was not certified by peer review) is the author/funder, who has granted medRxiv a license to display the preprint in perpetuity.
It is made available under a CC-BY-NC 4.0 International license .

algorithmic, both deterministic or with randomness and also incorporate heuristic elements. All these possible methods differ in their computational requirements and their performance can always be compared in terms of the final value for the objective function they manage to reach. Computationally intensive methods, however, rapidly bring in limitations to conduct e.g. sensitivity analysis or Monte Carlo simulations of the model parameters for increased confidence as they require long computing times per single parameter set evaluation. Taking this into consideration, a computationally inexpensive heuristic optimisation method, based on the R number and groups mortalities, was devised in view of the simulation results obtained by other more computational intense methods.

Heuristic R-based optimum path (HRBOP) strategy for vaccination

A heuristic R-based optimum path (HRBOP) strategy was developed that establishes the vaccination priority at any given time on the group with the highest projected mortality per infection avoided via vaccination. That mortality is however accounted from two sources and not only from the group's itself, the projected secondary and subsequent infections inflicted on the entire population by the avoided infection in the group, are also estimated and accounted for.

Under the HRBOP strategy, priority is directed at any given moment to the vaccination of the group *i* with the highest number of projected avoidable deaths per vaccination (see Eq. 1). This is calculated as a function of three elements, namely (i) the risk of infection in that group (as the ratio of the rate of infections and the number of individuals in the group); (ii) the mortality per infection in the group ($f_{d_ni}^{i}$) and (iii) the projected secondary and subsequent infections an infected group member would inflict on the entire population.

If the R number is accepted as a good estimator of infection propagation at a given moment, the last term (the projected secondary infections) can be estimated if group-specific detailed information about the ongoing R number is available such that a matrix of R numbers between groups (R_M) can be built. This matrix can then be projected to any number of infection cycles (n) by powering the matrix to n.

All these three terms could therefore in principle be measured or estimated from actual data directly collected by the health systems in a community, making no model required to apply the HRBOP strategy.

The calculation of the projected avoidable deaths for all population groups (**PAD_v**), in terms of the model variables, is presented in Eq. 1 (see also Appendix). Eq. 1 was used to evaluate the HRBOP method against the alternatives for the case study example for Spain. A value of three infection cycles (n=3) was used.

$$\mathbf{PAD_v} = (\mathbf{r_{i_h}} ./ \mathbf{N_{sv}}) .* [\mathbf{R_{M(9x9)}}^{n} + \mathbf{I_{(9x9)}}] * \mathbf{f_{d_ni}} \qquad \text{(Eq. 1)}$$

where $\mathbf{I}_{(9x9)}$ is the identity matrix of the indicated size.

Although the HRBOP strategy is demonstrated here on the dynamic model, its practical implementation does not require or rely on any model, partly decoupling the outcome sequence of priority groups from possible model shortcomings and uncertainties.

Used in conjunction with a dynamic model, the HRBOP method is computationally inexpensive as it runs in one single model simulation through its so-called optimum path. There is no requirement for repeated model simulations to evaluate the objective function for changes in vaccination sequence. The computational low cost allows for its use in conjunction with sensitivity and Monte Carlo simulations of the vaccination sequence outcome against uncertain model parameters.

medRxiv preprint doi: https://doi.org/10.1101/2020.10.12.20211094; this version posted October 14, 2020. The copyright holder for this preprint (which was not certified by peer review) is the author/funder, who has granted medRxiv a license to display the preprint in perpetuity.
It is made available under a CC-BY-NC 4.0 International license .

A final advantage of the low computational requirement of the HRBOP method is that it allows for its deployment together with the model on low cost web-based platforms, making a vaccination optimisation method available globally at no cost.

Comparison of vaccine distribution strategies (case study for Spain)

Five different strategies for vaccination of the population are evaluated for comparison for a case example using the population demographics and epidemiological data from Spain, namely:

i) No group prioritisation: all population in all groups is called for vaccination in equal terms.

ii) Priority to the groups with the highest mortality per infection (from highest to lowest). Groups are called one by one and only once until coverage for each group is reached (single call)

iii) Priority to the groups with the highest number of interactions (daily contacts) (from highest to lowest). Groups are called one by one and only once until coverage is reached (single call).

iv) HRBOP strategy (heuristic R-based optimum vaccination path). Groups can be called for a period and be recalled at later stages more than one time with flexibility partial group vaccination.

v) The best of all the possible sequences of groups priority. Groups are called one by one and only once until coverage is reached. This apporach requires intensive computation as all the possible combinations between all groups need to be evaluated (9! = 362,880 simulations)

The parameters as shown in Table S1 and Tables S3.a-b were used with the following initial conditions and assumptions:

- No pre-existing immunity, (i.e. $N_{ir}^{ini} = 0$).
- No initial vaccinated individuals and fatalities.
- Initial case incidence of 0.1% for NI and S and 0.3% for PS respect to the entire population.
- All remaining population initially considered as healthy susceptible (H).
- A total population of 47,026,208 as for Spain in 2019 is considered.
- Constant rate of vaccination of 1% of the population per day until campaign ends.
- Different vaccine effectiveness and maximum population coverage are evaluated.

Figure 3 shows the results for the five strategies, in terms of proposed sequence of priority groups for vaccination as well as the progression in total fatalities and R number with time, for a vaccine effectiveness of 75% and a maximum population coverage of 80%. A summary of all results obtained for nine combinations of these two parameters is presented in Table 1.

Table 1. Performance results of different strategies for vaccine distribution at different vaccine effectiveness and coverage of the population.

Vaccine Effectiveness	Maximum Population Coverage	No Prioritisation by Groups (Final fatalities)	Highest-to-Lowest Mortality	Most-to-Least Interactions	Heuristic R-based Path	Best of All Possible Sequences	Lowest fatalities achieved (Final fatalities)
			(Percentage change in fatalities)				
100%	95%	42,494	15.8%	-61.9%	-65.2%	-72.0%	11,915
100%	80%	42,692	16.5%	-63.1%	-64.6%	-71.6%	12,142
100%	50%	45,254	36.2%	-55.3%	-55.9%	-59.7%	18,244
75%	95%	70,998	12.1%	-65.4%	-65.6%	-73.8%	18,582
75%	**80%**	**71,265**	**11.6%**	**-63.5%**	**-64.0%**	**-71.7%**	**20,150**
75%	50%	74,942	19.2%	-45.2%	-45.7%	-50.3%	37,215
50%	95%	109,867	6.0%	-40.6%	-41.0%	-52.7%	51,954
50%	80%	110,138	5.4%	-36.6%	-37.2%	-46.8%	58,607
50%	50%	113,998	8.5%	-21.6%	-21.9%	-26.0%	84,342

medRxiv preprint doi: https://doi.org/10.1101/2020.10.12.20211094; this version posted October 14, 2020. The copyright holder for this preprint (which was not certified by peer review) is the author/funder, who has granted medRxiv a license to display the preprint in perpetuity.
It is made available under a CC-BY-NC 4.0 International license .

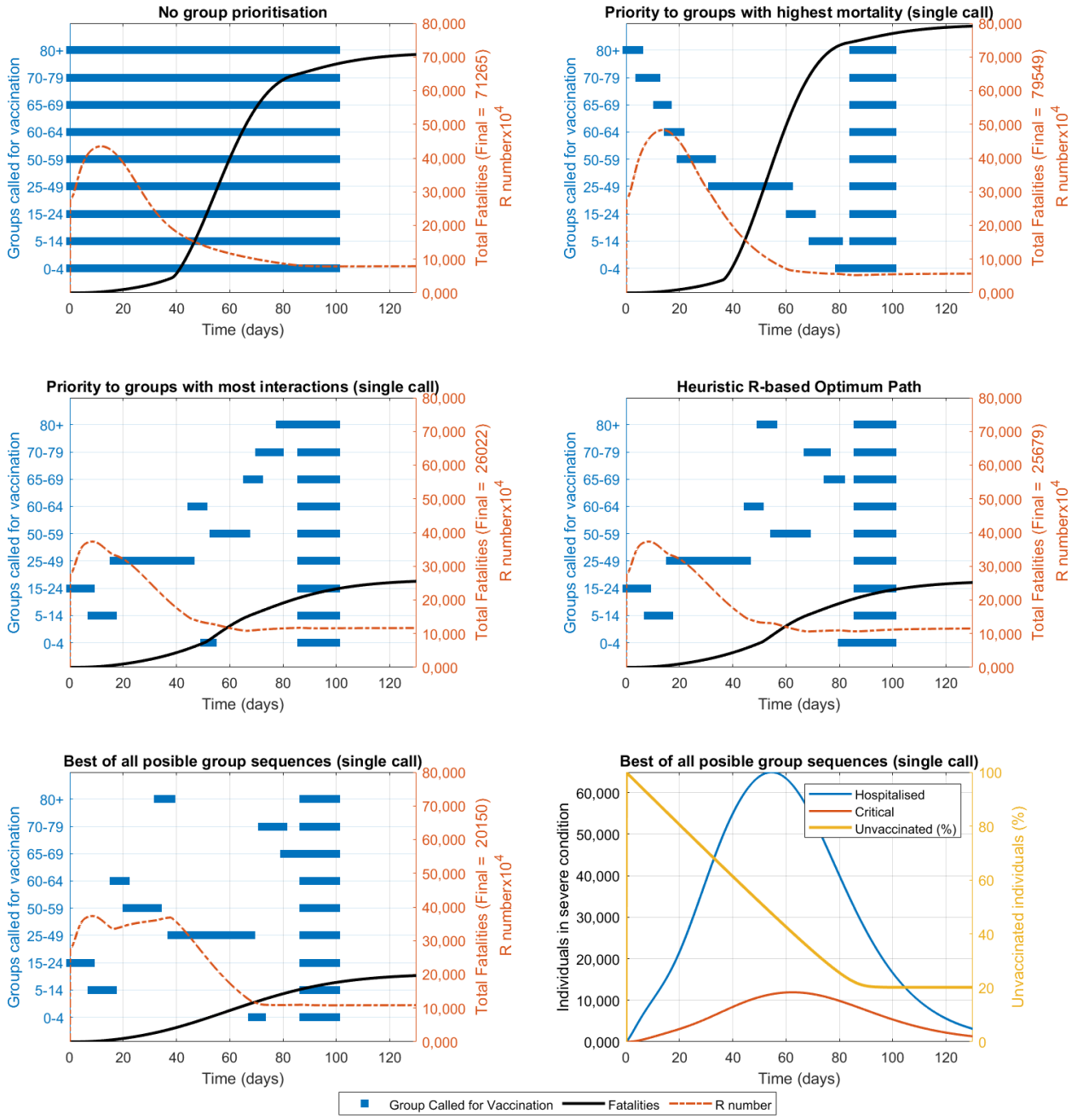

Figure 3. Compared vaccination strategies showing active groups called for vaccination, fatalities and R value over time for the case study with data and demographics from Spain. Constant vaccination rate is set at 1% of the total population per day, vaccine effectiveness is 75% and population coverage is 80%. The best result was obtained after (computationally intensive) evaluation of all possible group sequences (assuming only one single call per group). The computationally inexpensive heuristic R-based optimum path is evaluated for weekly cycles and allows for multiple partial calls to any specific group.

The different strategies proposed lead to very different and significant impacts respect to the baseline number of predicted fatalities if no group prioritisation is implemented. If a strategy based on priority to the groups with the highest mortality is followed, the predicted total number of fatalities actually increases significantly (~12% higher). On the contrary, if priority is established to those groups with the most interactions (from highest to lowest), dramatic reductions in fatalities (~63% lower) are predicted (Table 1). If the optimum strategy is further refined using the HRBOP

medRxiv preprint doi: https://doi.org/10.1101/2020.10.12.20211094; this version posted October 14, 2020. The copyright holder for this preprint (which was not certified by peer review) is the author/funder, who has granted medRxiv a license to display the preprint in perpetuity.
It is made available under a CC-BY-NC 4.0 International license .

method, additional smaller improvements can be achieved. Finally if intensive computational resources are available the best of all possible (single group call) sequences among all possible ones can be sought using a model. In this case, the best result was obtained in this manner (~72% lower number of fatalities). The HRBOP and the best of all sequences found differ very little from the one of groups from highest to lowest number of interactions. This trend of reductions and differences between the strategies remains consistent for different vaccine effectiveness and population coverage values (Table 1). The detailed simulation results analogous to those in Figure 3 for all combinations are presented in Figures S1-9 in the Supplementary Information.

It is important to note that the above results strongly indicate that in principle, and independently from the availability of a calibrated model and computational resources, following a strategy of priority to population groups with the most interactions or a similar more refined sequence obtained by the HRBOP method, can achieve enormous reductions in total fatalities at the end of the vaccination campaign.

Conclusions

The dynamic deterministic model developed, describing individuals in (age-segregated) population groups and disease stages, can be applied to the evaluation of vaccination strategies. The model results appear to describe expected trends and allow for deep mechanistic analyses to draw hypotheses and conclusions that can inform public health policy.

Our results strongly suggest that a planned vaccine distribution following prioritised sequences of population groups can achieve enormous reductions is the final number of fatalities at the end of the vaccination campaign. Based on the results we strongly advice against a group prioritisation criterion based on mortality only that ignores the group's level of interaction with others. The criteria of priority to those groups with the highest number of interactions (daily person to person contacts) appears as the one with the highest immediate payoff in terms of reduction of the final number of fatalities. The computationally-inexpensive model-independent heuristic R-based optimum path method proposed achieved moderate improvements on the final number of fatalities respect to the prioritisation strategy of highest to lowest interactions. Both these strategies do not differ by much from the model-based computationally-intensive evaluation of the best group priority sequence among all possible ones.

medRxiv preprint doi: https://doi.org/10.1101/2020.10.12.20211094; this version posted October 14, 2020. The copyright holder for this preprint (which was not certified by peer review) is the author/funder, who has granted medRxiv a license to display the preprint in perpetuity.
It is made available under a CC-BY-NC 4.0 International license .

Appendix - Dynamic COVID-19 model description

The definition of the model dynamic (state) variables is shown in Table A1. Each variable corresponds to the number of individuals in that stage in a vector per (age-related) population group (9 activity groups as defined above). Under this structure, each dynamic variable is a vector of dimension 1x9, and the total number of states is a matrix of dimensions 15x9 (15 stages and 9 population groups). Vector variables and parameters are represented in bold font and scalar ones in regular font across all the manuscript.

Table A1. Model dynamic variables accounting for the number of individuals in each infection stage and group.

Definition "Number of individuals…"	**Vector per group** (1x15 vector)	**Total from all groups**
Healthy susceptible to infection	$\mathbf{N_h}$	N_{hT}
Non-infectious pre-symptomatic	$\mathbf{N_{ni}}$	N_{niT}
Infectious pre-symptomatic	$\mathbf{N_{ps}}$	N_{psT}
Infectious symptomatic	$\mathbf{N_s}$	N_{sT}
Requiring hospitalisation	$\mathbf{N_{sh}}$	N_{shT}
Requiring critical care	$\mathbf{N_{sc}}$	N_{scT}
Recovered & immune	$\mathbf{N_{ir}}$	N_{irT}
Vaccinated still susceptible to infection	$\mathbf{N_h^v}$	N_{hvT}
Vaccinated Non-infectious pre-symptomatic	$\mathbf{N_{ni}^v}$	N_{nivT}
Vaccinated Infectious pre-symptomatic	$\mathbf{N_{ps}^v}$	N_{psvT}
Vaccinated Infectious symptomatic	$\mathbf{N_s^v}$	N_{svT}
Vaccinated Requiring hospitalisation	$\mathbf{N_{sh}^v}$	N_{shvT}
Vaccinated Requiring critical care	$\mathbf{N_{sc}^v}$	N_{scvT}
Vaccinated immune	$\mathbf{N_i^v}$	N_{ivT}
Deceased	$\mathbf{N_d}$	N_{dT}

Rates of transition between infection stages

The progression of individuals across stages, as illustrated in Figure 1, includes the impact of vaccination bringing individuals directly into an immune stage or, if ineffectively vaccinated, remaining in their current stage. The transitions between stages are governed by the rates of infection, disease transition and vaccination shown in Table A2. All the rates are in vectors with each element corresponding to the rate for each age-related population group.

The average rates of transition between stages are defined as per the latest epidemiological and clinical data and they can be updated as knowledge of the disease increases and treatments improve. These parameters include the proportion of individuals that transition to a more severe stage or recover (Table A3) and the average times reported at each stage before transition or recovery (Table A4).

medRxiv preprint doi: https://doi.org/10.1101/2020.10.12.20211094; this version posted October 14, 2020. The copyright holder for this preprint (which was not certified by peer review) is the author/funder, who has granted medRxiv a license to display the preprint in perpetuity.
It is made available under a CC-BY-NC 4.0 International license .

Table A2. Rates of infection and transition between states in vectors per population group.

Definition "Rate of …"	Variable	Units
Infection by interaction with infectious pre-symptomatic	r_{i_ps}	# H infected/day
Infection by interaction with infectious symptomatic	r_{i_s}	# H infected/day
Transition from non-infectious to infectious pre-symptomatic	r_{ps_ni}	# NI to PS / day
Transition from pre-symptomatic to symptomatic	r_{s_ps}	# PS to S / day
Transition from symptomatic to hospitalised	r_{sh_s}	# S to SH / day
Transition from hospitalised to critical	r_{sc_sh}	# SH to SC / day
Transition from critical to deceased	r_{d_sc}	# SC to D / day
Recovery from pre-symptomatic non-infectious	r_{r_ni}	# NI to R / day
Recovery from pre-symptomatic infectious	r_{r_ps}	# PS to R / day
Recovery from symptomatic	r_{r_s}	# S to R / day
Recovery from hospitalised	r_{r_sh}	# SH to R / day
Recovery from critical	r_{r_sc}	# SC to R / day
Vaccination of healthy susceptible	r_{v_h}	# H to HV / day
Vaccination of infected non-infectious	r_{v_ni}	# NI to NIV / day
Vaccination of infected pre-symptomatic	r_{v_ps}	# PS to PSV / day
Vaccination of recovered & already immune	r_{v_ir}	# IR to IV / day

Table A3. Fractions of individuals progressing through each severity stage per population group.

Definition		Parameter	Units
Fraction of NI that will become PS		f_{ps_ni}	#PS/#NI
Fraction of PS that will become S		f_{s_ps}	#S/#PS
Fraction of S that will become SH		f_{sh_s}	#SH/#S
Fraction of SH that will become SC		f_{sc_sh}	#SC/#SH
Fraction of cared SC that will die into D		f_{d_sc}	#D/#SC_{IC}
Fraction of NI that will recover into R[1]	(1- f_{ps_ni})	f_{r_ni}	#IR/#NI
Fraction of PS that will recover into R[1]	(1- f_{s_ps})	f_{r_ps}	#IR/#PS
Fraction of S that will recover into R[1]	(1- f_{sh_s})	f_{r_s}	#IR/#S
Fraction of SH that will recover into R[1]	(1- f_{sc_sh})	f_{r_sh}	#IR/#SH
Fraction of cared SC that will recover into R[1]	(1- f_{d_sc})	f_{r_sc}	#IR/#SC_{IC}

[1]Calculated by difference with the complementary, not an input parameter

medRxiv preprint doi: https://doi.org/10.1101/2020.10.12.20211094; this version posted October 14, 2020. The copyright holder for this preprint (which was not certified by peer review) is the author/funder, who has granted medRxiv a license to display the preprint in perpetuity.
It is made available under a CC-BY-NC 4.0 International license .

Table A4. Clinical average times in each infection stage in vectors per population group.

Definition	Parameter	Units
Time to become infectious after infection	$\mathbf{t}_{ps_ni}$	days
Time to develop symptoms from becoming infectious	$\mathbf{t}_{s_ps}$	days
Time to require hospitalisation from symptoms onset	$\mathbf{t}_{sh_s}$	days
Time to require critical care from hospitalisation	$\mathbf{t}_{sc_sh}$	days
Time to death from critical condition	$\mathbf{t}_{d_sc}$	days
Time to death from critical if no care is available	$\mathbf{t}_{d_nc}$	days
Time to fully recover from presymptomatic non-infectious	$\mathbf{t}_{r_ni}$	days
Time to fully recover from presymptomatic infectious	$\mathbf{t}_{r_ps}$	days
Time to fully recover from (non-severe) symptoms	$\mathbf{t}_{r_s}$	days
Time to fully recover from hospitalisation	$\mathbf{t}_{r_sh}$	days
Time to fully recover from critical condition	$\mathbf{t}_{r_sc}$	days

The rates of transition between stages (in number of individuals per day) are described in Eqs. A1.a-e. All rates are vectors per age group of dimensions (1x9). Note that the point operators between vectors indicate an element-by-element vector operation.

$$\mathbf{r}_{ni_h} = \mathbf{r}_{i_ps} .+ \mathbf{r}_{i_s} \quad \text{(Eq. A1.a)}$$

$$\mathbf{r}_{ps_ni} = (\mathbf{f}_{ps_ni} ./ \mathbf{t}_{ps_ni}) .* \mathbf{N}_{ni} \quad \text{(Eq. A1.b)}$$

$$\mathbf{r}_{s_ps} = (\mathbf{f}_{s_ps} ./ \mathbf{t}_{s_ps}) .* \mathbf{N}_{ps} \quad \text{(Eq. A1.c)}$$

$$\mathbf{r}_{sh_s} = (\mathbf{f}_{sh_s} ./ \mathbf{t}_{sh_s}) .* \mathbf{N}_{s} \quad \text{(Eq. A1.d)}$$

$$\mathbf{r}_{sc_sh} = (\mathbf{f}_{sc_sh} ./ \mathbf{t}_{sc_sh}) .* \mathbf{N}_{sh} \quad \text{(Eq. A1.e)}$$

The rates of individuals fully recovering and becoming immune from the different infected stages (in number of individuals per day) are described in Eqs A2.a-e. (all rates in vectors per age group).

$$\mathbf{r}_{r_ni} = (\mathbf{f}_{r_ni} ./ \mathbf{t}_{r_ni}) .* \mathbf{N}_{ni} \quad \text{(Eq. A2.a)}$$

$$\mathbf{r}_{r_ps} = (\mathbf{f}_{r_ps} ./ \mathbf{t}_{r_ps}) .* \mathbf{N}_{ps} \quad \text{(Eq. A2.b)}$$

$$\mathbf{r}_{r_s} = (\mathbf{f}_{r_s} ./ \mathbf{t}_{r_s}) .* \mathbf{N}_{s} \quad \text{(Eq. A2.c)}$$

$$\mathbf{r}_{r_sh} = (\mathbf{f}_{r_sh} ./ \mathbf{t}_{r_sh}) .* \mathbf{N}_{sh} \quad \text{(Eq. A2.d)}$$

$$\mathbf{r}_{r_sc} = (\mathbf{f}_{r_sc} ./ \mathbf{t}_{r_sc}) .* \mathbf{N}_{sc_ic} \quad \text{(Eq. A2.e)}$$

The rate of transition from critical to deceased is the sum of that of those in critical condition receiving intensive care ($\mathbf{r}_{d_scic}$) plus that of those without available care ($\mathbf{r}_{d_scnc}$) as per Eqs. A3.a-c. All critical individuals not receiving intensive care ($\mathbf{N}_{sc_ncc}$) are assumed to become fatalities after a time ($\mathbf{t}_{d_nc}$). A description of the critical care model allocation (in case the ICU capacity limits is reached) is provided below.

$$\mathbf{r}_{d_sc} = \mathbf{r}_{d_scic} + \mathbf{r}_{d_scnc} \quad \text{(Eq. A3.a)}$$

where

$$\mathbf{r}_{d_scic} = (\mathbf{f}_{d_sc} ./ \mathbf{t}_{d_sc}) .* \mathbf{N}_{sc_ic} \quad \text{(Eq. A3.b)}$$

$$\mathbf{r}_{d_scnc} = (1 ./ \mathbf{t}_{d_nc}) .* \mathbf{N}_{sc_ncc} \quad \text{(Eq. A3.c)}$$

medRxiv preprint doi: https://doi.org/10.1101/2020.10.12.20211094; this version posted October 14, 2020. The copyright holder for this preprint (which was not certified by peer review) is the author/funder, who has granted medRxiv a license to display the preprint in perpetuity.
It is made available under a CC-BY-NC 4.0 International license .

Allocation of critical care capacity if exceeded

The impact of available critical care capacity is modelled by a specific function to allocate critically ill individuals as per the available ICU. The function allocates critically ill individuals in two possible groups, namely those admitted to ICU ($\mathbf{N_{sc_ic}}$) and those not admitted to ICU due to lack of capacity or for medical or humanitarian reasons ($\mathbf{N_{sc_ncc}}$). At each simulation time point the allocation function is computed for the total $\mathbf{N_{sc}}$ per age group.

The function allocates ICU resources with priority to populations groups with higher ICU survival rate (f_{r_sc}) until the maximum number of intensive care units is reached leaving any remaining individuals without care, in this way $\mathbf{N_{sc_ic}}$ and $\mathbf{N_{sc_ncc}}$ are computed.

As the COVID-19 outbreak has progressed, data indicate that not all patients in critical condition have been admitted into intensive care units (ICU). Data show that many individuals with very poor prognosis, particularly those of oldest age may have never been referred to ICU due to capacity limitations or other medical humanitarian reasons. Data from Spain (Ministerio Sanidad España: Act. 107 COVID-19) show that for individuals over 70, only a fraction of the reported fatalities previously hospitalised was ever admitted to ICU and this may not be only due to ICU lack of capacity. In order to maintain consistency with the reported data (Ministerio Sanidad España: Act. 107 COVID-19) the parameters of f_{d_sc} and f_{sc_sh} have been estimated such that the product of $f_{d_sc} * f_{sc_sh}$ (fatality ratios over hospitalised individuals) is consistent with reported numbers for all ages irrespective of reported ICU admissions.

Rates of infection

The infection of healthy susceptible individuals (H and HV) is modelled as occurring only via their interaction with infectious either pre-symptomatic (PS) or symptomatic (S) individuals. Hospitalised (SH) and critical (SC) individuals are assumed not available for contacts neither are those deceased (D). Immune individuals after recovery (IR) or effective vaccination (IV) are also not infectious but contribute to the interactive pool of individuals towards herd immunity.

Two rates of infection of healthy susceptible individuals (in number of infections per day) are defined, one from each one of the two possible infecting groups (PS and S). However, in order to serve the goal of determining the optimal sequence of vaccination through population groups, the rates of infection have been expanded into terms for each population group.

The rate of infection of each (age-related) population group i results from the product of the number of healthy susceptible (H) individuals in the group (N_h^i) times the sum of the rates of infection from contacts with each one of all the groups. This, for each group, is the product of the average number of daily contacts with individuals of that group ($ni_h^{i,j}$) times the fraction of those in that group which are infectious (PS or S) times the likelihood of contagion to occur (modelled as function of the use of protection measures e.g. PPE by individuals in *i* and *j* groups) (see Eqs A4.a-b and Figure A1).

$$r_{i_ps}^i = N_h^i * \Sigma_j(ni_h^{i,j}.* f_{ips}^j.*p_{ips}^{i,j}) \qquad \text{(Eq. A4.a)}$$

$$r_{i_s}^i = N_h^i * \Sigma_j(ni_h^{i,j}.* f_{is}^j.*p_{is}^{i,j}) \qquad \text{(Eq. A4.b)}$$

medRxiv preprint doi: https://doi.org/10.1101/2020.10.12.20211094; this version posted October 14, 2020. The copyright holder for this preprint (which was not certified by peer review) is the author/funder, who has granted medRxiv a license to display the preprint in perpetuity.
It is made available under a CC-BY-NC 4.0 International license .

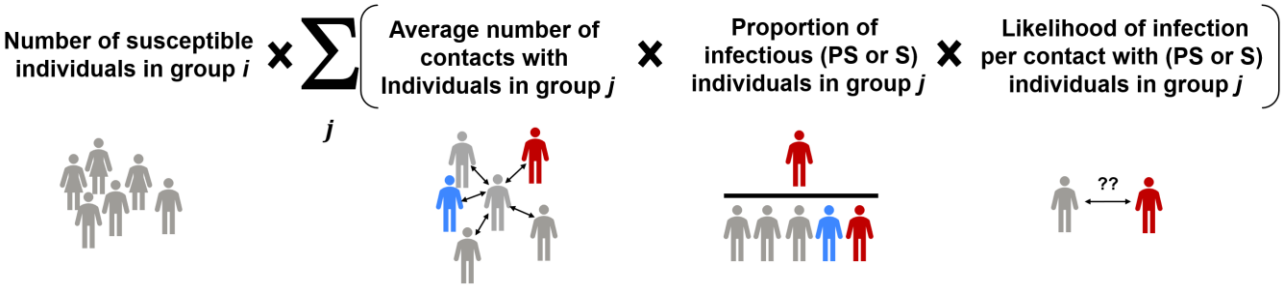

Figure A1. Visualisation of the rate of infection of individuals from a group *i* as per Eq. A4

For each (age-related) group, the *average number of daily contacts* an individual in a group *i* has with individuals from each one of the groups *j* ($ni_{i,j}$) are the most important parameters required as an input as they describe the level of social interactivity. These inputs allow for the description of specific key activities in a given group as well as for a complete customisation to the specifics of any community or country. Recent data from contact tracing applications and modelling makes the use of these information possible and reliable for these parameters (Prem *et al*., 2020). Examples on how these parameters reflect interventions is the opening of schools, which would involve high numbers of daily contacts between children in schools age groups, similarly for secondary school or universities but not necessarily with the other groups. This mapping of contacts is provided via a contacts matrix, in which only the part above the diagonal can be provided as direct input while the part below the diagonal is automatically calculated for consistency between groups based on their relative population sizes. Table S3b shows an example of values arbitrarily assigned and using the demographics of Spain 2019 (INE Spain, 2020). Interventions such as the *degree of social isolation* as described by Rodríguez *et al*.(2020) remain possible to simulate by modification of these matrix of average daily contacts even at a more detailed level since specific values for group-to-group number of daily contacts can be defined.

The second term impacting the rate of infection of a group *i* is, for each *j* group with which contacts exist, the *proportion of individuals that are infectious* (i.e. PS and S) and still interacting (f_{ips}^j and f_{is}^j). This can be directly computed at every time step from the dynamic variables (Eq. A5). This computation incorporates the impact of the *awareness of infection* after positive testing (Rodríguez *et al*., 2020) via a reduction factor of social interaction for those infected-aware (due to positive testing) or of infected-suspicious individuals. For untested individuals in a group *j* showing symptoms (S), a precautionary self or imposed partial quarantine is captured by the parameter (rfi_s^j). For tested individuals, the awareness of infection after a positive result is assumed to lead to a full quarantine and removes those individuals from regular interaction with others. The fractions of infectious PS and S individuals that remain in interaction with others (f_{ips} and f_{is}) are calculated as per Eqs A5.a-b. Hospitalised, critical and deceased are considered excluded from the pool of interacting individuals.

$$f_{ips}^j = (1-pt_{ps}^j * t_{sns_ps}) \quad * N'^j_{ps} / [N'^j_h + N'^j_{ni} + (1-pt_{ps}^j * t_{sns_ps}) * N'^j_{ps} + (1-pt_s^j * t_{sns_s}) * rfi_s^j * N'^j_s) + N'^j_{ir} + N'^j_{iv}] \quad \text{(Eq. A5.a)}$$

$$f_{is}^j = (1-pt_s^j * t_{sns_s}) * rfi_s^j * N'^j_s) / [N'^j_h + N'^j_{ni} + (1-pt_{ps}^j * t_{sns_ps}) * N'^j_{ps} + (1-pt_s^j * t_{sns_s}) * rfi_s^j * N'^j_s) + N'^j_{ir} + N'^j_{iv}] \quad \text{(Eq. A5.b)}$$

where, N'^j_x means the sum in stage x of both those not vaccinated and those ineffectively vaccinated ($N'^j_x = N_x^j + N_{xv}^j$) in population group *j*; pt_{ps}^j is the proportion of randomly tested non-symptomatic individuals and pt_s^j is the proportion of symptomatic individuals tested. The parameters t_{sns_ps} and t_{sns_s} refer to the sensitivity of the tests for individuals in PS and S stages respectively. The differences are justified since e.g. for non-symptomatic individuals, only RT-qPCR tests are typically assumed adequate while, for symptomatic S individuals, both RT-qPCR and serological tests are used.

The third term impacting the rate of infection within group *i*, is the *likelihood of infection per contact with an infectious* (PS or S) individual of the group *j*. This is an element that could be directly

medRxiv preprint doi: https://doi.org/10.1101/2020.10.12.20211094; this version posted October 14, 2020. The copyright holder for this preprint (which was not certified by peer review) is the author/funder, who has granted medRxiv a license to display the preprint in perpetuity.
It is made available under a CC-BY-NC 4.0 International license .

provided in the form of matrix of likelihood of infection between groups (**p_{i_ps}** and **p_{i_s}**) without further modelling. If the effect of specific interventions if of interest, the likelihood of infection can be further modelled in more detail as per below.

In this example likelihood of infection between groups is presented modelled as per Eq. A6a-b based on the *level of PPE use and awareness* displayed by the two interacting parties (Rodríguez *et al*., 2020) (see Eqs. A6) together with a newly proposed degree of infectiousness for PS and S. The parameters inf_{ps} and inf_s reflect the degree of infectiousness between 0 and 1. This degree of infectiousness is considered potentially relevant in view not only on possible differences in viral load between PS and S individuals but also of ongoing research regarding specific population groups (e.g. children) which could display different levels of infectiousness to others. The level of protection and awareness of healthy susceptible individuals in the group *i* is described by the parameter lpa_h^i as they interact with infectious PS and S individuals of group *j* with lpa_{ps}^j and lpa_s^j respectively. The values of the parameters can vary between 0 and 1, with 1 corresponding to the use of comprehensive protective measures and zero to the most careless opposite situation. Different values are assigned for the different activity and age-related population groups. (e.g. for primary school children and elderly). In this way, for individuals in group *i*, the likelihood of infection per interaction with individuals of the group *j* (PS and S respectively) is calculated as per Eqs A6.a-b.

$$p_{i_ps}^{ij} = (1 - lpa_h^i) * (1 - lpa_{ps}^j) * inf_{ps}^j; \qquad \text{(Eq. A6.a)}$$

$$p_{i_s}^{ij} = (1 - lpa_h^i) * (1 - lpa_s^j) * inf_s^j; \qquad \text{(Eq. A6.b)}$$

Table A5 shows the definitions and units of key variables and parameter used in the calculation of the rate of infection.

Table A5. Behaviour-related variables and parameters affecting the rate of infection.

Definition	Parameter	Units
Average daily contacts per H group *i* individual with *j*	ni_h^{ij}	#contacts *j*/ H individual *i*·day
Personal protection and awareness by H in group *i*[1]	lpa_h^i	Ø
Personal protection and awareness by PS in group *j*[1]	lpa_{ps}^j	Ø
Personal protection and awareness by S in group *j*[1]	lpa_s^j	Ø
Infectiousness level by PS in group *j*[1]	inf_{ps}^j	Ø
Infectiousness level by S in group *j*[1]	inf_s^j	Ø
Likelihood of infection by H individual *i* with PS in *j*[2]	$p_{i_ps}^{ij}$	infections / *i* contacting PS in *j*
Likelihood of infection by H individual *i* with S in *j*[2]	$p_{i_s}^{ij}$	infections / *i* contacting PS in *j*
Percentage of tested individuals from PS in group *j*[1]	pt_{ps}^j	#random (non S) tested/#(H+NI+PS)
Percentage of tested individuals from S in group *j*[1]	pt_s^j	#random S tested/#S
Sensitivity of tests used on PS individuals	t_{sns_ps}	#PS detected / #PS tested
Sensitivity of tests used on S individuals	t_{sns_s}	#S detected / #S tested
Reduction factor in contacts by S in group *j*[1]	rfi_s^j	Ø

[1]Values only within the interval [0,1]; [2]Calculated if modelled or they can be directly provided as input parameters.

medRxiv preprint doi: https://doi.org/10.1101/2020.10.12.20211094; this version posted October 14, 2020. The copyright holder for this preprint (which was not certified by peer review) is the author/funder, who has granted medRxiv a license to display the preprint in perpetuity.
It is made available under a CC-BY-NC 4.0 International license .

Rate of vaccination

Once an effective vaccination against the SARS-CoV-2 virus becomes available, its mass deployment will take place, at any given moment, at a specific vaccination rate. This rate will be limited either by the availability of vaccine doses or by the system's capacity to deliver them.

The recipients of the vaccine within the population groups will be all those individuals, either non tested or having tested (truly or falsely) negative or having recovered, that display no symptoms. This will include the vaccinations to the target healthy individuals (H) but also to untargeted individuals such as the non infectious (NI), those unaware (untested or with false negative test) that are pre-symptomatic infectious (PS) and those that have recovered from the infection (aware or not) (R).

A total capacity vaccination rate is defined (r_v^T), in number of individuals that can be vaccinated per day. The vaccination rates of individuals in each of the four possible stages suitable for vaccination, are defined as per Eqs A7.a-d in vectors for each (age-related) population group. The rate is proportional to the individuals in each stage and in each group among those suitable and called for vaccination.

$$\mathbf{r_{v_h}} = r_v^T * \boldsymbol{f_v} .* \mathbf{N_{sv}} / \Sigma_i (\boldsymbol{f_v} .* \mathbf{N_{sv}})] .* \mathbf{N_h} ./ \mathbf{N_{sv}} \qquad \text{(Eq. A7.a)}$$

$$\mathbf{r_{v_ni}} = r_v^T * \boldsymbol{f_v} .* \mathbf{N_{sv}} / \Sigma_i (\boldsymbol{f_v} .* \mathbf{N_{sv}})] .* \mathbf{N_{ni}} ./ \mathbf{N_{sv}} \qquad \text{(Eq. A7.b)}$$

$$\mathbf{r_{v_ps}} = r_v^T * \boldsymbol{f_v} .* \mathbf{N_{sv}} / \Sigma_i (\boldsymbol{f_v} .* \mathbf{N_{sv}})] .* \mathbf{N^{\#}_{ps}} ./ \mathbf{N_{sv}} \qquad \text{(Eq. A7.c)}$$

$$\mathbf{r_{v_ir}} = r_v^T * \boldsymbol{f_v} .* \mathbf{N_{sv}} / \Sigma_i (\boldsymbol{f_v} .* \mathbf{N_{sv}})] .* \mathbf{N_{ir}} ./ \mathbf{N_{sv}} \qquad \text{(Eq. A7.d)}$$

where f_v is a vector of zeros with one only on the groups currently called for vaccination in a specific moment. $\mathbf{N^{\#}_{ps}}$ refers to untested PS individuals therefore unaware of their infection and susceptible of receiving vaccination $\mathbf{N^{\#}_{ps}} = (1\text{-}\mathbf{pt_{ps}}.* t_{sns_ps}).*\mathbf{N_{ps}}$.

In a given population group that no distinction is assumed possible between individuals in the vaccination suitable stages without symptoms. Therefore, in a population group *i*, the total number of undistinguishable individuals suitable for vaccination (N_{SV}^i) is given by Eq. A7.d.

$$N_{SV}^i = N_h^i + N_{ni}^i + (1-pt_{ps}^j * t_{sns_ps}) * N_{ps}^j + N_r^i \qquad \text{(Eq. A7.d)}$$

With the above definition, the problem of determining the optimum plan for vaccine application is reduced to the determination, at any given moment in time, of the optimum values of f_v^i for each population group, until the vaccination campaign is completed.

Dynamic transition equations

The dynamic variation on the number of unvaccinated individuals in each stage over time in vectors of (age-related) population groups is governed by the population balance equations Eqs A8.a-g.

$$d\mathbf{N_h}/dt = -\mathbf{r_{ni_h}} .*(\mathbf{1\text{-}pV_h}) - \mathbf{r_{v_h}} \qquad \text{(Eq. A8.a)}$$

$$d\mathbf{N_{ni}}/dt = \mathbf{r_{ni_h}} .*(\mathbf{1\text{-}pV_h}) - (\mathbf{r_{ps_ni}} + \mathbf{r_{r_ni}}) .*(\mathbf{1\text{-}pV_{ni}}) - \mathbf{r_{v_ni}} \qquad \text{(Eq. A8.b)}$$

$$d\mathbf{N_{ps}}/dt = \mathbf{r_{ps_ni}} .*(\mathbf{1\text{-}pV_{ni}}) - (\mathbf{r_{s_ps}} + \mathbf{r_{r_ps}}) .*(\mathbf{1\text{-}pV_{ps}}) - \mathbf{r_{v_ps}} \qquad \text{(Eq. A8.c)}$$

$$d\mathbf{N_s}/dt = \mathbf{r_{s_ps}} .*(\mathbf{1\text{-}pV_{ps}}) - (\mathbf{r_{sh_s}} + \mathbf{r_{r_s}}) .*(\mathbf{1\text{-}pV_s}) \qquad \text{(Eq. A8.d)}$$

$$d\mathbf{N_{sh}}/dt = \mathbf{r_{sh_s}} .*(\mathbf{1\text{-}pV_s}) - (\mathbf{r_{sc_sh}} + \mathbf{r_{r_sh}}) .*(\mathbf{1\text{-}pV_{sh}}) \qquad \text{(Eq. A8.e)}$$

$$d\mathbf{N_{sc}}/dt = \mathbf{r_{sc_sh}} .*(\mathbf{1\text{-}pV_{sh}}) - (\mathbf{r_{d_sc}} + \mathbf{r_{r_sc}}) .*(\mathbf{1\text{-}pV_{sc}}) \qquad \text{(Eq. A8.f)}$$

$$d\mathbf{N_{ir}}/dt = \mathbf{r_{r_ni}} .*(\mathbf{1\text{-}pV_{ni}}) + \mathbf{r_{r_ps}}.*(\mathbf{1\text{-}pV_{ps}}) + \mathbf{r_{r_s}} .*(\mathbf{1\text{-}pV_s}) + \ldots$$
$$\mathbf{r_{r_sh}} .*(\mathbf{1\text{-}pV_{sh}}) + \mathbf{r_{r_sc}} .*(\mathbf{1\text{-}pV_{sc}}) + \mathbf{r_{v_r}} \qquad \text{(Eq. A8.g)}$$

medRxiv preprint doi: https://doi.org/10.1101/2020.10.12.20211094; this version posted October 14, 2020. The copyright holder for this preprint (which was not certified by peer review) is the author/funder, who has granted medRxiv a license to display the preprint in perpetuity.
It is made available under a CC-BY-NC 4.0 International license .

The vaccines once commercialised will likely display a given effectiveness (**eV**) per population group, which will lead to a proportion of ineffective vaccinations. Those ineffectively vaccinated individuals will not acquire immunity and therefore remain susceptible to infection and to all stages of severity. These must however be accounted for separately as they should not be vaccinated again. The population balances for all vaccinated individuals in their possible stages are presented in Eqs A8.h-n.

$$d\mathbf{N_h^v}/dt = -\mathbf{r_{ni_h}} .* \mathbf{pV_h} - \mathbf{r_{v_h}}.*(1-\mathbf{eV}) \quad \text{(Eq. A8.h)}$$

$$d\mathbf{N_{ni}^v}/dt = \mathbf{r_{ni_h}} .* \mathbf{pV_h} - (\mathbf{r_{ps_ni}} + \mathbf{r_{r_ni}}) .* \mathbf{pV_{ni}} - \mathbf{r_{v_ni}} \quad \text{(Eq. A8.i)}$$

$$d\mathbf{N_{ps}^v}/dt = \mathbf{r_{ps_ni}} .* \mathbf{pV_{ni}} - (\mathbf{r_{s_ps}} + \mathbf{r_{r_ps}}) .* \mathbf{pV_{ps}} - \mathbf{r_{v_ps}} \quad \text{(Eq. A8.j)}$$

$$d\mathbf{N_s^v}/dt = \mathbf{r_{s_ps}} .* \mathbf{pV_{ps}} - (\mathbf{r_{sh_s}} + \mathbf{r_{r_s}}) .* \mathbf{pV_s} \quad \text{(Eq. A8.k)}$$

$$d\mathbf{N_{sh}^v}/dt = \mathbf{r_{sh_s}} .* \mathbf{pV_s} - (\mathbf{r_{sc_sh}} + \mathbf{r_{r_sh}}) .* \mathbf{pV_{sh}} \quad \text{(Eq. A8.l)}$$

$$d\mathbf{N_{sc}^v}/dt = \mathbf{r_{sc_sh}} .* \mathbf{pV_{sh}} - (\mathbf{r_{d_sc}} + \mathbf{r_{r_sc}}) .* \mathbf{pV_{sc}} \quad \text{(Eq. A8.m)}$$

$$d\mathbf{N_i^v}/dt = \mathbf{r_{r_ni}} .*\mathbf{pV_{ni}} + \mathbf{r_{r_ps}}.*\mathbf{pV_{ps}} + \mathbf{r_{r_s}} .*\mathbf{pV_s} + \ldots \mathbf{r_{r_sh}} .*\mathbf{pV_{sh}} + \mathbf{r_{r_sc}} .*\mathbf{pV_{sc}} + \mathbf{r_{v_r}} - \mathbf{r_{v_h}}.* \mathbf{eV} \quad \text{(Eq. A8.n)}$$

Finally the balance of fatalities is shown in Eq. A8.o.

$$d\mathbf{N_d}/dt = \mathbf{r_{d_sc}} \quad \text{(Eq. A8.o)}$$

where $\mathbf{pV_\#}$ is the proportion of individuals in stage # (vector for each population group) that have received a vaccine dose (effective or not).

Computation of the dynamic reproduction number (R)

The reproduction number describes the potential infections of susceptible individuals from infected individuals (Delamater *et al*. 2019). Since the model generates a deterministic set of values for its outputs at any given time, an instantaneous deterministic computation of the reproduction number (R) is possible. Multiple parameters and variables influence the R such as the duration of the infectious stages; the likelihoods of infection per contact as well as the percentages of individuals transitioning between stages.

The dynamic reproduction number (R) is computed over time according to Eq. A9 from the current values of the model state variables. The computation of R assumes that infectious individuals can only infect others while they are in pre-symptomatic (PS) and symptomatic (S) stages. Although it has been speculated that post-symptomatic recovered individuals may be infectious for some period of time, this has not been considered at this time given the insufficient data. Hospitalised and critical individuals are assumed not able to infect others in the general population as they are in controlled settings. The provided dynamic output of the reproduction number R provides additional information that can be used for decision making.

The computation of the R number is conducted considering that infected individuals can take only three possible infectious paths, namely: (i) Recovery after a period as pre-symtomatic (PS → R); (ii) Recovery after periods as presymtomatic and symptomatic (PS → S → R) and (iii) Hospitalisation after periods as presymtomatic and symptomatic (PS → S → SH). These paths are made of combinations of four possible infectious stage intervals in which infected individuals spend time and can infect others at their corresponding infection rate (see Table A6).

medRxiv preprint doi: https://doi.org/10.1101/2020.10.12.20211094; this version posted October 14, 2020. The copyright holder for this preprint (which was not certified by peer review) is the author/funder, who has granted medRxiv a license to display the preprint in perpetuity.
It is made available under a CC-BY-NC 4.0 International license .

Table A6. Possible infectious stages intervals for the R number computation.

Infectious interval	Fraction of infected passing the interval (ind_{interv}/ind_{inf})	Interval duration (d)	Total infections per stage interval per individual infected (inf_{interv}/ind_{inf})
PS → R	$\mathbf{f_{r_ps}}$	$\mathbf{t_{r_ps}}$	$(r_{i_psT}/ N_{psT})* \mathbf{t_{r_ps}} .* \mathbf{f_{r_ps}}$
PS → S	$(1 - \mathbf{f_{r_ps}})$	$\mathbf{t_{s_ps}}$	$(r_{i_psT}/ N_{psT})* \mathbf{t_{s_ps}} .* (1 - \mathbf{f_{r_ps}})$
S → R	$(1 - \mathbf{f_{r_ps}})* \mathbf{f_{r_s}}$	$\mathbf{t_{r_s}}$	$(r_{i_sT} / N_{sT}) * \mathbf{t_{r_s}} .* (1 - \mathbf{f_{r_ps}}) .* \mathbf{f_{r_s}}$
S → SH	$(1 - \mathbf{f_{r_ps}})* (1 - \mathbf{f_{r_s}})$	$\mathbf{t_{sh_s}}$	$(r_{i_sT} / N_{sT}) * \mathbf{t_{sh_s}} .* (1 - \mathbf{f_{r_ps}}) .* (1 - \mathbf{f_{r_s}})$

The dynamic computation of R results from adding the total infection contributions of the four stage intervals as shown in Eq. A9.

$$R_t = \Sigma\, [(r_{i_psT} / N_{psT})* (\mathbf{t_{r_ps}} .* \mathbf{f_{r_ps}} + \mathbf{t_{s_ps}} .* (1 - \mathbf{f_{r_ps}})) + (r_{i_sT} / N_{sT}) * (\mathbf{t_{r_s}} .* (1 - \mathbf{f_{r_ps}}).* \mathbf{f_{r_s}} + \mathbf{t_{sh_s}} .* (1 - \mathbf{f_{r_ps}}).*(1 - \mathbf{f_{r_s}}))\,] \quad \text{(Eq. A9)}$$

in which, the population group weighted average rates of infection by PS and S are given as per Eqs. A10a-b.

$$r_{i_psT} = \Sigma\, (\mathbf{r_{i_ps}} .*\mathbf{N'_{ps}})/N'_{psT}) \qquad [inf_{PS}/ind_{PS}\cdot d] \qquad \text{(Eq. A10.a)}$$

$$r_{i_sT} = \Sigma\, (\mathbf{r_{i_s}} .* \mathbf{N'_s}) /N'_{sT}) \qquad [inf_{S}/ind_{S}\cdot d] \qquad \text{(Eq. A10.b)}$$

where, N'^{j}_{x} means the sum in stage x of both those unvaccinated and those ineffectively vaccinated ($\mathbf{N'_x} = \mathbf{N_x} + \mathbf{N_{xv}}$) for all population groups.

Source code

The Matlab® source code and the Excel files containing all inputs and parameters used are fully available on demand.

Acknowledgements

Khalifa University (Grant 8474000317 CRPA-2020-SEHA) and the Government of Abu Dhabi for the funding and infrastructure provided.

References

Bendix A. (2020) A day-by-day breakdown of coronavirus symptoms shows how the disease, COVID-19, goes from bad to worse. Business Insider (last accessed 30-3-2020) *https://www.businessinsider.com/coronavirus-covid19-day-by-day-symptoms-patients-2020-2*

Bubar, K.M., Kissler, S.M., Lipsitch, M., Cobey, S., Grad, Y., Larremore, D.B., 2020. Model-informed COVID-19 vaccine prioritization strategies by age and serostatus. medRxiv 2020.09.08.20190629. https://doi.org/10.1101/2020.09.08.20190629

Cori A, Ferguson NM, Fraser C & Cauchemez S. A new framework and software to estimate time-varying reproduction numbers during epidemics. *American Journal of Epidemiology*, 2013; 178(9):1505–1512 (https://doi.org/10.1093/aje/kwt133).

Delamater, P. L., Street, E. J., Leslie, T. F., Yang, Y., & Jacobsen, K. H. (2019). Complexity of the Basic Reproduction Number (R_0). *Emerging Infectious Diseases*, 25(1), 1-4. *https://dx.doi.org/10.3201/eid2501.171901.*

Emanuel EJ, Persad G, Kern A, Buchanan A, Fabre C, Halliday D, Heath J,Herzog L, Leland RJ, Lemango ET, Luna F, McCoy MS, Norheim OF,Ottersen T, Schaefer GO, Tan KC, Wellman CH, Wolff J, Richardson HS. An ethical framework for global vaccine allocation. *Science*, 369(6509):1309-1312

medRxiv preprint doi: https://doi.org/10.1101/2020.10.12.20211094; this version posted October 14, 2020. The copyright holder for this preprint **(which was not certified by peer review)** is the author/funder, who has granted medRxiv a license to display the preprint in perpetuity.
It is made available under a CC-BY-NC 4.0 International license .

Field RI, Caplan AL.(2012) Evidence-based decision making for vaccines: the need for an ethical foundation. *Vaccine*. 30(6):1009-1013. DOI: 10.1016/j.vaccine.2011.12.053

Gatto, M., Bertuzzo, E., Mari, L., Miccoli, S., Carraro, L., Casagrandi, R., Rinaldo, A., 2020. Spread and dynamics of the COVID-19 epidemic in Italy: Effects of emergency containment measures. PNAS 117, 10484–10491. https://doi.org/10.1073/pnas.2004978117

Giordano, G., Blanchini, F., Bruno, R., Colaneri, P., Filippo, A.D., Matteo, A.D., Colaneri, M., 2020. Modelling the COVID-19 epidemic and implementation of population-wide interventions in Italy. Nat Med 1–6. https://doi.org/10.1038/s41591-020-0883-7

Hellewell, J., Abbott, S., Gimma, A., Bosse, N.I., Jarvis, C.I., Russell, T.W., Munday, J.D., Kucharski, A.J., Edmunds, W.J., Sun, F., Flasche, S., Quilty, B.J., Davies, N., Liu, Y., Clifford, S., Klepac, P., Jit, M., Diamond, C., Gibbs, H., Zandvoort, K. van, Funk, S., Eggo, R.M., 2020. Feasibility of controlling COVID-19 outbreaks by isolation of cases and contacts. The Lancet Global Health 8, e488–e496. https://doi.org/10.1016/S2214-109X(20)30074-7

INE Spain (2020) *https://www.ine.es/* (last accessed31/3/2020)

Pollán M. *et al*. (2020) Prevalence of SARS-CoV-2 in Spain (ENE-COVID): a nationwide, population-based seroepidemiological study. *Lancet* https://doi.org/10.1016/S0140-6736(20)31483-5

JHCRC (2020) John Hopkins – Coronavirus Resource Center (https://coronavirus.jhu.edu/map.html)

Krammer, F.(2020) SARS-CoV-2 vaccines in development. *Nature*. https://doi.org/10.1038/s41586-020-2798-3

Kissler, S.M., Tedijanto, C., Goldstein, E., Grad, Y.H., Lipsitch, M., 2020. Projecting the transmission dynamics of SARS-CoV-2 through the postpandemic period. Science. https://doi.org/10.1126/science.abb5793

Kucharski, A.J., Russell, T.W., Diamond, C., Liu, Y., Edmunds, J., Funk, S., Eggo, R.M., Sun, F., Jit, M., Munday, J.D., Davies, N., Gimma, A., Zandvoort, K. van, Gibbs, H., Hellewell, J., Jarvis, C.I., Clifford, S., Quilty, B.J., Bosse, N.I., Abbott, S., Klepac, P., Flasche, S., 2020. Early dynamics of transmission and control of COVID-19: a mathematical modelling study. The Lancet Infectious Diseases. https://doi.org/10.1016/S1473-3099(20)30144-4

Lauer, S.A., Grantz, K.H., Bi, Q., Jones, F.K., Zheng, Q., Meredith, H.R., Azman, A.S., Reich, N.G. and Lessler, J. (2020). The incubation period of coronavirus disease 2019 (COVID-19) from publicly reported confirmed cases: estimation and application. Annals of internal medicine.

Liu, Yangzi; Salwi, Sanjana; Drolet, Brian C. Multivalue ethical framework for fair global allocation of a COVID-19 vaccine. *J Med Ethics* ; 46(8): 499-501, 2020 08.

Matrajt, L., Eaton, J., Leung, T., Brown, E.R., 2020. Vaccine optimization for COVID-19, who to vaccinate first? medRxiv 2020.08.14.20175257. https://doi.org/10.1101/2020.08.14.20175257

Mello MM, Silverman RD, Omer SB. Ensuring Uptake of Vaccines against SARS-CoV-2. N Engl J Med 2020; 383:1296-1299 DOI: 10.1056/NEJMp2020926

Ministerio de Sanidad de España. Actualización nº67: enfermedad por SARS-CoV-2 (COVID-19) 03.04.2020 *https://www.mscbs.gob.es/profesionales/saludPublica/ccayes/alertasActual/nCov-China/documentos/Actualizacion_74_COVID-19.pdf*

Nishiura H, Kobayashi T, Suzuki A, Jung S-Mok, Hayashi K, Kinoshita R, Yang Y, Yuan B, Akhmetzhanov AR, Linton NM, Miyama T (2020) Estimation of the asymptomatic ratio of novel coronavirus infections (COVID-19), *International Journal of Infectious Diseases*, *doi:https://doi.org/10.1016/j.ijid.2020.03.020*

Nishiura H, Linton NM, Akhmetzhanov AR. Serial interval of novel coronaviru)s (COVID-19) infections. International Journal of Infectious Diseases 2020; 93:284-286 (https://doi.org/10.1016/j.ijid.2020.02.060).

Parker, E.P.K., Shrotri, M. & Kampmann, B. Keeping track of the SARS-CoV-2 vaccine pipeline. Nat Rev Immunol (2020). https://doi.org/10.1038/s41577-020-00455-1

Prem K, van Zandvoort K, Klepac P, Eggo RM, Davies NG, Centre for the Mathematical Modelling of Infectious Diseases COVID-19 Working Group, Cook AR, Jit M. (2020) Projecting contact matrices in 177 geographical regions: an update and comparison with empirical data for the COVID-19 era *medRxiv* 2020.07.22.20159772

medRxiv preprint doi: https://doi.org/10.1101/2020.10.12.20211094; this version posted October 14, 2020. The copyright holder for this preprint **(which was not certified by peer review)** is the author/funder, who has granted medRxiv a license to display the preprint in perpetuity.
It is made available under a CC-BY-NC 4.0 International license .

Rodríguez J., Uratani JM Patón M. and Acuña JM (2020) Modelling the impact of interventions on the progress of the COVID-19 outbreak including age segregation. MedRxiv https://www.medrxiv.org/content/10.1101/2020.04.04.20053017v3

Roosa, K., Lee, Y., Luo, R., Kirpich, A., Rothenberg, R., Hyman, J.M., Yan, P., Chowell, G., 2020. Real-time forecasts of the COVID-19 epidemic in China from February 5th to February 24th, 2020. Infectious Disease Modelling 5, 256–263. https://doi.org/10.1016/j.idm.2020.02.002

Schwartz J.L. (2020). Evaluating and Deploying Covid-19 Vaccines — The Importance of Transparency, Scientific Integrity, and Public Trust. NEJM DOI: 10.1056/NEJMp2026393

Wang, X., Peng, H., Shi, B., Jiang, D., Zhang, S., Chen, B., 2019. Optimal vaccination strategy of a constrained time-varying SEIR epidemic model. Communications in Nonlinear Science and Numerical Simulation 67, 37–48. https://doi.org/10.1016/j.cnsns.2018.07.003

Wearing HJ, Rohani P, Keeling MJ (2005) Appropriate Models for the Management of Infectious Diseases. *PLoS Med* 2(7): e174. https://doi.org/10.1371/journal.pmed.0020174

WHO (2020a). Access to COVID-19 tools (act) accelerator: A Global Collaboration to Accelerate the Development, Production and Equitable Access to New COVID-19 diagnostics, therapeutics and vaccines. (*https://www.who.int/publications/m/item/access-to-covid-19-tools-(act)-accelerator*)

WHO 2020b. Public health criteria to adjust public health and social measures in the context of COVID-19 Annex to Considerations in adjusting public health and social measures in the context of COVID-19. Geneva: World Health Organization; 2020 (https://www.who.int/publications/i/item/public-health-criteria-to-adjust-public-health-and-social-measures-in-the-context-of-covid-19).

Wilder, B., Charpignon, M., Killian, J.A., Ou, H.-C., Mate, A., Jabbari, S., Perrault, A., Desai, A.N., Tambe, M., Majumder, M.S., 2020. Modeling between-population variation in COVID-19 dynamics in Hubei, Lombardy, and New York City. PNAS. https://doi.org/10.1073/pnas.2010651117

Yu, Z., Liu, J., Wang, X., Zhu, X., Wang, D., Han, G., 2016. Efficient Vaccine Distribution Based on a Hybrid Compartmental Model. PLOS ONE 11, e0155416. https://doi.org/10.1371/journal.pone.0155416

Zhou F, Yu T, Du R, *et al*. (2020) Clinical course and risk factors for mortality of adult inpatients with COVID-19 in Wuhan, China: a retrospective cohort study. *Lancet* published online March 9. *http://dx.doi.org/10.1016/S0140-6736(20)30566-3.*